Environmental Aging and Deadhesion of Polyimide Dielectric Films

Steven Murray, Craig Hillman, and Michael Pecht

CALCE Electronic Products and Systems Center

Department of Mechanical Engineering

University of Maryland

College Park, Maryland, 20742, USA

ABSTRACT

One possible failure mechanism of products containing polyimide dielectric is deadhesion of polyimide from neighboring metallization. Deadhesion usually occurs due to the combined damage mechanisms of environmental aging and fatigue. In this paper, the rate of aging of Kapton-E polyimide is quantified as a function of temperature and humidity exposure using peel and tensile tests. An accelerated test methodology that accounts for both aging and fatigue and that can be used to evaluate the resistance of electronic products to polyimide deadhesion is then proposed.

KEYWORDS

Polyimide, polymer aging, adhesion, delamination, reliability, accelerated testing

1. INTRODUCTION

A common failure mechanism of polyimide dielectric is deadhesion by aging-assisted fatigue. Fatigue crack growth results from thermo-mechanical and hygroscopic stresses induced by changes in the temperature and humidity of the local environment [1,2], as well as from any mechanically applied loading such as bending or vibration. Environmental aging results from the simultaneous processes of hydrolysis and thermo-oxidative degradation, which are rate-determined by the average level of temperature and humidity of the local environment [3-23]. Aging results in decreased strength and embrittlement of polyimide, and increases the crack growth rate under fatigue loading.

Current qualification methods used in industry focus on fatigue characterization through thermal cycling alone, and neglect the deleterious effects that environmental aging has on the fatigue life of polymers [24-28]. In order to account for aging in accelerated tests, a model is needed that quantifies it and explains how it can be accelerated. Previous work studied polyimide aging using high-temperature aging tests and calculated an activation energy for thermo-oxidative degradation for use in an Arrhenius model, or performed aging on samples which were immersed in water and calculated an activation energy for hydrolysis. Moisture concentration could not be varied in such studies, such that the effect of this variable on the rate of aging was not considered. In this study, a methodology to characterize the rate of polyimide aging as a function of both temperature and humidity using peel and tensile tests is proposed. Empirical models for the aging of Kapton-E[1] polyimide film with titanium barrier metallization, as well as unmetallized Kapton-E polyimide film, are then developed. These aging models can be used in combination with fatigue testing to design accelerated tests for product qualification.

2. ADHESION OF POLYIMIDE DIELECTRIC

In order to build a circuit, traces of conductive material are be made on top of the polyimide, or between alternating layers of polyimide. Copper is the most common material for interconnects, although other metals such as aluminum have also been used. Barrier/adhesion layers consisting of a secondary reactive metal such as titanium or chromium are often used between copper and dielectric material in order

[1] Kapton is a trademark of E. I. du Pont de Nemours and Company.

to prevent copper from diffusing into polyimide and to provide protection against corrosion. Adhesion between polyimide and metallization results from van-der-Waals forces, mechanical interlocking, and the formation of metal-polymer complexes (chemical bonding) with the barrier metallization [15,29-32]. Adhesion of polyimide to itself, in contrast, is due to cross-linking, chain tangling, van-der-Waals forces, and acid-base interactions [15].

Plasma treatment of polyimide is commonly used prior to metal deposition in order to improve the adhesion of the polyimide to the metallization. Adhesion is improved through the removal of surface contamination, chemical modification of the polyimide that creates active groups available for bonding to the metallization, and texturing of the polyimide surface that results in greater mechanical interlocking between the materials [20].

3. DEADHESION OF POLYIMIDE DIELECTRIC

In order to operate reliably, the materials in a metal-polyimide multi-layer structure must stay adhered together throughout the life of the product. Deadhesion can result in impedance changes between transmission lines, as well as increased susceptibility to via fracture, corrosion, and conductive filament formation. Metal-polyimide interfacial strength exceeds that of the bulk polyimide when plasma pre-treatment of polyimide is performed and barrier metallization is used, such that deadhesion occurs by crack propagation through the bulk of the polyimide dielectric in the near-interface region [17-21,23].

Product failure can also occur due to the formation of cracks within bulk polyimide as the material becomes more brittle with aging. For example, cracks in polyimide wire insulation resulting from aging, through which electrical arcs could pass, have been blamed for the crashes of TWA flight 800 off Long Island in 1996, and Swissair flight 111 near Nova Scotia in 1998 [11].

3.1 Polyimide aging

The primary environmental aging mechanisms of polyimide are hydrolysis and thermo-oxidative degradation [8]. Polyimide film becomes more rigid and brittle during aging, and breaks at lower stresses and ultimate elongations [5-10]. Aging of metallized polyimides decreases the peel strength of the metallization [16,18-21].

Hydrolysis is the chemical reaction of a compound with water, resulting in the formation of one or more new compounds. Hydrolysis is generally the dominant aging mechanism at low temperatures due to its lower activation energy (approximately one-tenth that of thermo-oxidative degradation) in the early stages of the aging process. Degradation occurs rapidly in the early stages of aging, and then slows as the number of susceptible sites in the polymer chain decrease. The hydrolysis of polyimides is believed to occur by scission of the amide bond [8], and activation energies found for the reaction range from 13.2 kcal/mol (0.57 eV) [6] to 16.0 kcal/mol (0.69 eV) [7]. Strong acids (pH < 2) and strong bases (pH > 12) make the imide linkages susceptible to hydrolysis in addition to the amide linkages [7], resulting in additional damage to the polymer. Most damage due to hydrolysis can be recovered through high-temperature (i.e., >300ºC) heat treatment [22,23]. Since most fielded products do not experience such high temperatures during their use, however, the damage resulting from hydrolysis must be considered permanent for such products, and accounted for in design and qualification activities.

After the amide linkages available for hydrolysis have been exhausted, or when the product is used at high temperatures that drive moisture out of the film, thermo-oxidative degradation becomes a significant part of the aging process. A number of reactions occur during thermo-oxidative degradation, including scission of macromolecules, cross-linking, repacking of polymer chains, and crystallization [8]. These reactions modify the chemical structure of the polymer and permanently change the properties of the film. Activation energies in the range of 130-180 kcal/mol (5.64-7.81 eV) have been reported [8].

Metals catalyze the aging of polyimide. When polyimide is used as a dielectric material where it is in contact with metal, the polymer in the near-interface region ages more rapidly than the polymer located in the bulk of the film [1,3,13,14]. Radiation can also slightly catalyze thermo-oxidative and hydrolytic degradation processes [9], although polyimides are among the most radiation-resistant polymers known [20]. In the absence of water or oxygen, radiation produces no degradation, and polyimide has been successfully used in both aerospace and nuclear power generation environments [9].

3.2 Stresses in multi-layer structures

The primary stresses acting on polyimide dielectric in most environments are residual stresses from processing, and thermal and hygroscopic stresses resulting from changes in the local environment or power

cycling. In some applications, such as flex circuits subject to repeated bending loads, mechanically applied loads may also be significant.

Residual stresses are generated both during manufacture of the film and during subsequent processing. Most stresses from processing arise from thermal mismatch generated when materials are cooled from high processing temperatures. These stresses are usually fairly uniform, with minimal gradients within layers. However, the presence of vias modifies the stress distribution seen in an actual product. Stresses can also arise during metal deposition due to diffusional effects. These stresses are called intrinsic stresses, and result from the elimination of defects within the metal that have an associated free volume, such as grain boundaries, vacancies, and interstitials [2]. Intrinsic stresses are usually non-uniform, with a gradient through the thickness of the film. Residual stresses from processing can cause plastic yielding and modify the stress profiles experienced during thermal cycling early in the life of a product. These stresses decay gradually over time due to stress relaxation, as polyimide is a visco-elastic material.

Thermo-mechanical stresses arise due to coefficient of thermal expansion (CTE) mismatch between adjacent layers. Both shear and normal stresses are generated. Stresses generally increase exponentially as distance from the neutral axis increases, with the largest stresses found near the edges of a structure [1]. However, the presence of vias in the structure can greatly complicate stress fields, making them harder to predict analytically. Manufacturing variabilities can also change the distribution of stresses. The processes used to manufacture preimidized polyimide films such as Kapton lead to a high degree of molecular orientation, with most molecules aligned in the plane of the film. As a result, the out-of-plane CTEs of polyimide films are larger than the in-plane CTEs. In-place CTEs in the machine and transverse directions also vary slightly, due to stretching that occurs during processing on rolls. For example, Pottiger [34] found 1-mil Kapton-H film to have CTEs of 25 ppm/°C in the in-plane transverse direction, 32 ppm/°C in the in-plane machine direction, and 117 ppm//°C in the out-of-plane direction. Although out-of-plane stresses can affect via reliability, it is the smaller in-plane stresses that most directly affect deadhesion. Polyimides are now available with in-plane CTEs more closely matched to copper, such as Kapton-E, which has in-plane CTEs of 12-16 ppm/°C [35,36].

Moisture absorption from the environment induces stresses due to hygroscopic swelling [37-39]. Polyimides are hydrophilic, due in part to the highly polar nature of polyimide. Kapton-H, for example,

can absorb in excess of two water molecules for every three polyimide repeat units [40]. Swelling of polyimide as it absorbs moisture is linearly related to the relative humidity of the surrounding air, where the proportionality constant is the coefficient of hygroscopic expansion (CHE). In-plane CHEs of polyimides range from 8.3-41.3 ppm/%RH, although polyimides that absorb more water than others do not necessarily have a higher CHE [38]. CHEs of 15.0 and 18.0 ppm/%RH have been measured for Kapton-H in the machine and transverse directions of Kapton-H film, respectively, while values of 12.1 and 8.3 ppm/%RH have been measured for Kapton-E [38]. The out-of-plane hygroscopic expansion of polyimide film is generally about four times larger than the in-plane expansion [39]. As moisture enters the polymer, compressive normal stresses build up around the edges where the moisture concentration is higher, balanced by tensile normal stresses in the center. At the same time, the swelling induces shear stresses, with a maximum value approximately a quarter of the distance into the material [41].

3.3 Fracture mechanics of deadhesion

Crack growth rates in polyimide are strongly related to the stress intensity factor, as defined by linear-elastic fracture mechanics [42]. However, changes in temperature or humidity change the free volume within the polymer, which in turn affects its mobility and succeptibility to crack growth. Temperature also affects properties because molecules become further apart as temperature increases, which decreases intermolecular forces holding molecules together [43], and because the time scale of the material increases (i.e., time-temperature superposition). Humidity also affects properties due to plasticization and hydrogen bonding. Popelar [44] has developed a modified form of the WLF equation to describe the dependence of crack growth rate upon temperature and humidity in unmetallized Kapton-H film.

Aging of polyimides decreases the fracture toughness and increases the rate of crack growth under applied loading. For a polyimide aged at 232 °C, crack growth rate doubled in the first 2000 hours of aging, increased by 30% from 2000 to 4000 hours, and increased by an additional 5% from 4000 to 6000 hours [12]. Aging was found to result in microcracks in the polyimide matrix, which lowered the fracture toughness of the material.

4. AGING EXPERIMENTS

Previous studies on polyimide aging primarily used high-temperature aging experiments to calculate an activation energy for use in an Arrhenius model, and neglected the effect of moisture concentration on the reaction rate. If moist aging conditions were tested at all, not enough conditions were included to allow for the construction of a viable regression model to calculate the rate of aging at other conditions. Such an effort was undertaken in this paper.

Since most electrical products are exposed to both moisture and oxygen, both hydrolysis and thermo-oxidative degradation occur simultaneously. Temperature, humidity, and oxygen concentration all affect the rate of aging. Since oxygen concentration is constant in most applications at a standard atmospheric concentration of oxygen, this variable was left constant in these experiments, and aging was quantified as a function of temperature and humidity only.

4.1 Metallized Kapton-E film

An aging study was first performed on metallized polyimide. Copper strips with titanium barrier metallization were deposited on oxygen-plasma-treated Kapton-E film, and the degradation in the peel strength of the strips with aging was measured. The model resulting from this study can be used to design accelerated aging tests for products containing Kapton-E polyimide dielectric manufacturing with oxygen plasma treatment and titanium barrier metallization.

4.1.1 Procedure

A sheet 25.4 μm thick Kapton-E film was attached to an alumina substrate with adhesive. Following oxygen plasma-treatment of the polyimide, 3.2 mm wide strips of metal were deposited (28 μm of Cu, with a 1 kÅ barrier layer of sputtered Ti). Individual square test coupons with 7 strips of metal each were then cut.

Degradation in adhesion strength of the metallization was measured using 180° peel tests. Coupons were aged in test chambers at 35°C/25%RH, 35°C/85%RH, 60°C/55%RH, 85°C/25%RH, 85°C/85%RH,

130°C/1%RH[2], and 130°C/85%RH. Peel strengths were measured at 0, 20, 275, 1000, and 2000 hours into the aging process at each aging condition. All peel tests were performed in a temperature and humidity controlled cleanroom, and coupons were stored in the cleanroom for 24 hours prior to testing to allow them to reach uniform moisture contents. A knife was used to peel up one edge of each metal strip. With the sample held in a vise, a wirebond pull tester was then used to peel back each strip at an angle of 180° and speed of 45 mm/min. Two peel strength measurements were taken for each strip, and the 14 measurements for each coupon were averaged and recorded. Three coupons were tested to obtain a baseline peel strength, and one coupon was tested at each subsequent data point. The peel test is illustrated in Fig. 1.

4.1.2 Results

Following peel testing, grazing angle Fourier Transform Inrared Spectroscopy (FTIR) and depth profiling by Secondary Ion Mass Spectroscopy (SIMS) were performed on the fracture surface. A layer of polyimide of approximately 150Å thickness was found on the back of the metal peel strips, indicating that the failure occurred cohesively within the polyimide. Peel strength decreased during aging, with both temperature and humidity affecting the rate of degradation. The peel strength was normalized by dividing the measured peel strength by the average peel strength at the baseline condition, such that the aging was tracked in terms of the percentage of the original peel strength remaining.

According to basic reaction kinetics theory, the rate of a chemical reaction increases with increasing reactant concentration by a power law, and with increasing temperature by an Arrhenius relation [45]. The general form of a rate equation is:

$$k = A \cdot [R_1]^B \cdot [R_2]^C \cdot e^{-D/T} \quad (1)$$

where A is a constant, $[R_x]$ are reactant concentrations, B and C are the constants representing the orders of the reaction with respect to those reactants, D is a constant calculated as the activation energy for the reaction divided by the universal gas constant, and T is the absolute temperature.

[2] Temperature and humidity were actively controlled by the test chambers for all conditions except for 1%RH tests, for which only temperature was controlled. The high temperatures of the test drive virtually all of the moisture out of the film. Since water is continuously produced as a product of thermo-oxidative degradation, however, the humidity was rounded up to 1% instead of down to 0% to reflect the fact that trace amounts of moisture would be present in the film continuously.

Polyimide degrades due to the simultaneous processes of hydrolysis and thermo-oxidative degradation. The rate of hydrolysis is dependent upon humidity by a power relation and dependent upon temperature by an Arrhenius relation. The rate of thermo-oxidative degradation is also dependent upon temperature by an Arrhenius relation, but is independent of humidity. The overall reaction rate can be expressed as:

$$k = A \cdot RH^{n} \cdot e^{-B/T} + C \cdot e^{-D/T} \tag{2}$$

where RH is the relative humidity expressed as a decimal between 0 and 1, T is the absolute temperature in K, and A, B, C, D, and n are constants. If the reaction is modeled as first-order with respect to humidity, n in Eq. (2) is set equal to 1.

The relation between peel strength and reaction rate must be determined next. The reaction rates are constant for each of the seven test conditions where temperature and humidity were held constant. When the natural logarithm of the normalized peel strength is graphed vs. the natural logarithm of aging time, straight lines are obtained for each aging condition. The normalized peel strengths therefore degrade by a power law in relation to time, instead of following first-order reaction kinetics (exponential decay)[3]. The aging equation can be written as:

$$P = 100 \cdot t^{-k} \tag{3}$$

where P is the normalized peel strength (% of original peel strength remaining), k is the reaction rate, and t is the time in hours.

With the general form of the model established, non-linear regression was used to solve for the model coefficients using the normalized tensile strength vs. time data. The resulting equation was:

$$P = 100 \cdot t^{-k} \tag{4a}$$

$$k = 4830 \cdot RH \cdot e^{-4020/T} + 36 \cdot e^{-2290/T} \tag{4b}$$

where P is the normalized peel strength and k is the reaction rate. Analysis of variance (ANOVA) found that the model fit the data with R^2=0.83. Variability in initial strength between coupons that resulted in scatter in the data was the largest contributor to the error in the fit. Graphs of the model overlaid on the original data are provided in Fig. 2.

[3] Data from previous aging studies performed by Bergstresser [4,6-7] using Kapton-E and chromium barrier metallization was analyzed for comparison. The peel strength vs. aging time curves from their data sets also became more linear when plotted on a log-log plot instead of a log plot, suggesting that a power function fits their data better than the more commonly used exponential function.

4.2 Unmetallized Kapton-E film

An aging study was also performed on unmetallized polyimide. The degradation in ultimate tensile strength of unmetallized, as-received Kapton-E film during aging was measured. In addition to helping to determine the effect of Ti metallization on the aging process, the resulting model could be used to design accelerated aging tests for products containing unmetallized polyimide.

4.2.1 Procedure

Dogbone-shaped samples were laser-cut from 25.4 μm thick Kapton-E film. Prior to testing, all samples were left out on racks in the laboratory for 24 hours to allow them to reach uniform moisture contents. Samples were then stretched until failure in a MTS Tytron micro-tensile tester, and their ultimate tensile strength and elongation at failure recorded. Tests were displacement-controlled at a rate of 10 mm/min, corresponding to speed C in ASTM test method D1708 [46] for plastic microtensile specimens. Since loads are applied gradually in most applications (thermal and moisture changes in the environment usually occur on a daily cycle), a low-speed test such as speed C is most representative of the actual application and was therefore chosen for use. For the baseline measurements, ten dogbone samples were tested, and the results averaged. For each subsequent data point, five dogbone samples were used.

Samples were aged at the same conditions as for the metallized Kapton-E peel test experiments, and tested at 0, 275, 1000, and 2000 hours into the aging process. Additional samples were aged at 150°C/85%RH and 175°C/1%RH for 275 and 750 hours, and at 300°C/1%RH for 20, 275, and 750 hours.

4.2.2 Results

Ultimate tensile strength decreased with aging, with both temperature and humidity affecting the rate of degradation. Degradation proceeded at a slower rate than with the metallized samples, with no statistically significant decrease noted at 1%RH conditions under 175°C and 85%RH conditions under 130°C within the duration of the test. To illustrate the degradation process, overlaid stress-strain curves for samples aged at 300°C/1%RH for different times are provided in Fig. 3. The material became more brittle with aging and fractured at lower stresses and strains, although no significant change in elastic modulus was noted. Tensile properties were normalized by dividing the measured property following aging by the

value of the property at the baseline condition, such that the aging was tracked in terms of the percentage of the original tensile property remaining.

When the natural logarithm of the ultimate tensile strength was graphed vs. time for each aging condition, straight lines were obtained. The tensile properties at each condition of temperature and humidity therefore degraded exponentially, per first order reaction kinetics. The aging equation can be written as:

$$S = 100 \cdot e^{-kt} \tag{5}$$

where S is the normalized ultimate tensile strength, k is the reaction rate, and t is the time in hours. The reaction rate is:

$$k = A \cdot RH \cdot e^{-B/T} + C \cdot e^{-D/T} \tag{6}$$

as was the case with the metallized samples.

Non-linear regression was used to solve for the model coefficients using the normalized tensile strength vs. time data. The resulting equation was:

$$S = 100 \cdot e^{-kt} \tag{7a}$$

$$k = 8.53 \cdot RH \cdot e^{-4510/T} + 600 \cdot e^{-7800/T} \tag{7b}$$

where P is the normalized ultimate tensile strength. ANOVA found that the model fit the data with R^2=0.95. Graphs of the model overlaid on the experimental data are provided in Fig. 4.

5. QUALIFICATION OF PRODUCTS CONTAINING POLYIMIDE

Reliability tests run by electronic product manufacturers generally are taken from industry or military standards. For example, the Institute for Interconnecting and Packaging Electronic Circuits (IPC), a leading standards authority for the printed circuit board industry [47], has several standards that detail tests than can be run to guarantee the quality and reliability of various product types [24-28]. Such test plans generally specify a temperature cycling test with a predefined cycle size and number of cycles, and sometimes specify a separate high temperature, high humidity aging test. Although such tests may be useful for supplier benchmarking and quality control purposes, they are inadequate for the qualification of products against material deadhesion. Shortcomings such test plans include:

- Effects of aging on fatigue resistance is neglected, as aging is not incorporated into the thermal cycling test, but is run separately, if at all.
- No correlation exists between the harshness and duration of the aging test and the application environment in which the product will be used.
- No correlation exists between the size and number of thermal cycles and the cycling that will be experienced in the application environment.
- Hygroscopic stresses due to humidity cycling in the application environment are neglected.

Additional testing would need to be performed to evaluate the reliability of a product in its application environment.

5.1 Test plan based on physics of failure

In order to evaluate the reliability of a product in its intended application environment, a qualification plan must take into account the damage mechanisms to which the product is susceptible, and the loads that the product will experience during its life. Five factors that affect the deadhesion of polyimide dielectric films are materials, product dimensions, manufacturing processing, aging, and applied stresses. Since it is assumed in accelerated test design that the materials, dimensions, and manufacturing processes used in for the test samples are the same as those that will be used for the actual product to be fielded, the two factors of primary importance for test design are aging and applied stresses. These factors in turn share the common sources of temperature and humidity. If present in the application, bending stresses or other mechanically applied loadings also need to be taken into account. A fishbone diagram summarizing these factors is provided in Fig. 5.

In most applications, the product would be exposed to both oxygen and water, and aging due to thermo-oxidative degradation and hydrolysis would be expected to occur simultaneously. If a damage model is available that quantifies the rate of aging at various intensities of temperature and humidity, an accelerated aging test can be designed to inflict an equivalent amount of damage in a shorter period of time by exposing a product to harsher conditions in the test. Eq. (4) is an example of such an aging model for the case of Kapton-E polyimide used with oxygen plasma treatment and titanium barrier metallization in an

environment with a standard atmospheric concentration of oxygen. A methodology similar to that used to develop this model could be used to quantify the aging of other materials.

The second mechanism contributing to deadhesion is fatigue. Crack growth rates vary depending upon the stress intensity factor, the mode mixity of the loading, the temperature and humidity of the local environment, and the amount of environmental aging that has occurred in the polyimide. If a damage model for material fatigue is available, the product qualification testing can be accelerated by using test cycles of a larger size than those encountered in the field. If no such model is available, time compression can be used for applied stresses. With this technique, the same number and magnitude of temperature and humidity cycles that would be encountered in the actual application are used in the test, but ramp rates and frequency of the cycles are increased. If non-hermetic product is being tested, dwell times should be long enough to allow for moisture absorption and desorption to occur at both the high and low ends of the cycles in order to capture the full effects of hygroscopic stresses.

To simulate the application environment in which aging and fatigue damage are incurred simultaneously, the aging in the test should be intermingled with the accumulation of fatigue damage. For some products, this can be accomplished using a single temperature/humidity cycling test with a large dwell time instituted on the high end of each cycle during which aging can occur, with the dwell time calculated using the aging model. If the product experiences bending, vibration, or shock during its life, these loads should also be applied intermittently throughout the temperature/humidity cycling test such that the damage induced by these loads are also distributed throughout the aging process. If a larger acceleration factor for aging is needed in order to obtain reasonable test lengths, as may occur when a product is being qualified for a long design life in a hot and damp environment, samples could be passed back and forth between a high temperature, high humidity HAST chamber and a temperature/humidity cycling chamber, such that when the test was completed, both an entire design lifetime of aging damage and fatigue damage had been accumulated by the product. If bending loads, shocks, or vibrations were also expected to be encountered in the application environment, then these loadings could be applied in series

with the temperature/humidity cycling. Such a test plan is illustrated in Fig. 6, where the fatigue loading is applied in three discrete phases throughout the aging process[4].

5.2 Calculation of aging test parameters

Tests must be designed such that overstress limits of the product are not exceeded. Examples of overstress limits are temperatures high enough that CTE mismatch stresses exceed material or interfacial strengths, and the glass transition temperatures any adhesives used in the product being qualified. Tests should be designed with as large an acceleration factor as possible to minimize the times required for testing, and test conditions are often chosen by setting load levels just below the overstress limits. Preliminary tests can be run if needed to help in identifying these limits.

The duration of time required for aging in a test can be determined by considering that a given percent degradation obtained in the application in time t_A (i.e., the design life for the product) and at rate k_T is equal to the percent degradation obtained in the test in time t_T and at rate k_T. Using Eq. (4a), for the case of Ti-metallized Kapton-E polyimide, this can be written as:

$$100t_A^{-k_A} = 100t_T^{-k_T} \tag{8}$$

Upon rearrangement, the test time can be calculated as:

$$t_T = t_A^{(k_A/k_T)} \tag{9}$$

where the reaction rates, k, are calculated using Eq. (4b). Since the chemistry of the aging process does not obey first-order reaction kinetics, the acceleration factor for the test can not be written in closed form, and straight-forward application of the Arrhenius equation to test design is invalid.

Aging times for unmetallized Kapton-E polyimide can be calculated in a similar manner. Using Eq. (7a):

$$100 \cdot e^{-k_A t_A} = 100 \cdot e^{-k_T t_T} \tag{10}$$

which upon rearrangement gives:

$$t_T = (k_A / k_T) t_A \tag{11}$$

[4] The number three was arbitrarily chosen. The use of a larger number of phases would make the test a better simulation of the application environment, but may complicate the test by requiring more manual handling of samples. Since aging is placed before fatigue, however, this simplification is conservative, and the test will be slightly more damaging to the product than the application environment.

where the reaction rates, k, are calculated using Eq. (7b).

5.3 Calculation of fatigue test parameters

For fatigue, time compression is recommended unless a damage model that relates cycle size to the crack growth rate is available. For time compression, the number and size of cycles is the same in the test as in the application environment. Ramp rates can be set to the maximum allowed by the chamber, so long as the thermal mass of the product is small and the product is not overly sensitive to thermal gradients. Dwells at the peaks should be long enough to allow for moisture absorption and desorption. If the high end of the cycle is also used for aging, then the dwell at the high end must be lengthened accordingly.

6. CONCLUSIONS

Models for the environmental aging of metallized Kapton-E polyimide and unmetallized Kapton-E polyimide have been developed. Both temperature and humidity were found to affect the rate of aging, and contacting metallization was found to catalyze the aging. The aging reaction for metallized polyimide was found to not obey first order reaction kinetics, invalidating the common practice of using a simple Arrhenius equation to model polymer aging for the case of metallized polyimides.

The methodologies presented could be used to develop aging models for other types of dielectric films. In the case of peel tests, however, future experimenters would be advised to measure peel strength by peeling one metal strip off of each of a number of test coupons at each data point, instead of peeling all of the strips off of one individual test coupon at each data point as was done on this test. Data would then be less sensitive to inter-coupon variations in initial adhesion strength due to manufacturing process variations, and the variation in the test would be reduced.

An accelerated testing methodology to evaluate the resistance of products to deadhesion that combines polymer aging with fatigue testing and captures the interactions between these two damage mechanisms has been proposed. Aging models can be used to design accelerated aging tests, which are combined with fatigue tests to qualify a product for a given application environment. This methodology overcomes some of the limitations of commonly used industry qualification techniques, and more accurately evaluates the resistance to deadhesion of products containing polyimide dielectric.

7. REFERENCES

[1] Suhir, E., 1988, "An Approximate Analysis of Stresses in Multilayered Elastic Thin Films," *ASME J. Appl. Mech*., **55**, pp. 143-148.

[2] Evans, A.G., and Hutchinson, J.W., 1995, "Overview No. 120: The Thermomechanical Integrity of Thin Films and Multilayers," *Acta Metal. Mater.*, **43**(7), pp. 2507-30.

[3] Anderson, S.G., Meyer, H.M., and Weaver, J.H., 1988, "Temperature-dependent X-ray Photoemission Studies of Metastable Co/Polyimide Interface Formation," *Journal of Vacuum Science & Technology A (Vacuum, Surfaces, and Films)*, **6**(4), pp. 2205-12.

[4] Arnold, C., and Borgman, L.K., 1971, "Chemistry and Kinetics of Polyimide Degradation," *American Chemical Society Polymer Preparations*, **12**(2), pp. 296-302.

[5] Askins, Robert D., 1983, "Hydrolytic Degradation of Kapton Film," report to Air Force, document AFWAL-TR-83-4125.

[6] Campbell, F.J., 1985, "Temperature Dependence of Hydrolysis of Polyimide Wire Insulation," *IEEE Transactions on Electrical Insulation*, **EI-20(1)**, pp. 111-6.

[7] DeIasi, R., and Russell, J., 1971, "Aqueous Degradation of Polyimides," *Journal of Applied Polymer Science*, **15**(12), pp. 2965-74.

[8] Bessonov, M.I., et al., 1987, *Polyimides: Thermally Stable Polymers*, Plenum Press, New York.

[9] DuPont, 1997, "Kapton Polyimide Film (Summary of Properties)," document 300874A.

[10] Turk, M.J., et al, 1999, "Evaluation of the Thermal Oxidative Stability of Polyimides via TGA Techniques," *Journal of Polymer Science: Part A – Polymer Chemistry*, **37**, pp. 3943-56.

[11] Furse, C., and Haupt, R., 2001, "Down to the Wire," *IEEE Spectrum*, **38**(2), pp. 34-9.

[12] Hutapea, P., and Yuan, F.G., 1999, "The Effect of Thermal Aging on the Mode-I Interlaminar Fracture Behavior of a High-Temperature IM7/LaRC-RP46 Composite," *Composites Science and Technology*, **59**(8), pp. 1271-86.

[13] Mittel, K.L., 1984, *Polyimides Synthesis, Characterization, and Application*, *Vol. 2*, Plenum Press, New York.

[14] Somasiri. N.L.D., R.L.D. Zenner, and Houge, J.C., 1991, "A Process for Surface Texturing of Kapton Polyimide to Improve Adhesion to Metals," *IEEE Transactions on Components, Hybrids, and Manufacturing Technology*, **14**(4), pp. 798-801.

[15] St. Clair, T.L., 1990, "Structure-Property Relationships in Linear Aromatic Polyimides," *Polyimides*, ed. D. Wilson, H.D. Stenzenberger, and P.M. Hergenrother, Blackie & Son, Glasgow, pp.58-78.

[16] Bergstresser, T.R., Bergkessel, N.E., and Poutasse, C.A., 1998, "Accelerated Humidity Durability Testing of Adhesiveless Polyimide Laminates," *Proceedings of the Fifth International Convention on Flex Circuits*, San Jose, CA.

[17] Bergstresser, T.R., et al, 1997, "Adhesion Performance of Polyimide Adhesiveless Flexible Laminates having Nickel Based Tiecoats," *Proceedings of the IPC Third Annual National Conference on Flex Circuits*, Phoenix, AZ.

[18] Bergstresser, T.R., et al, 1997, "Peel Strength of Adhesiveless Polyimide Laminates after Thermal and Chemical Exposure," *Proceedings of the Fourth International Conference on Flex Circuits*, Sunnyvale, CA.

[19] Bergstresser, T.R., et al, 1998, "The Effects of Moisture on Peel Strength of Adhesiveless Polyimide Laminates," *IPC Fourth Annual National Conference on Flexible Circuits: Meeting the Challenge of the Next Generation of Packaging*, San Jose, CA, vol. 2, pp. 63-71.

[20] Clearfield, H.M., Furman, B.K., and Callegari, T.A., 1994, "The Role of Physical and Chemical Structure in the Long-Term Durability of Metal/Polyimide Interfaces," *International Journal of Microcircuits and Electronic Packaging*, **17**(3), pp. 228-35.

[21] Girardeaux, C., Chambaud, G., and Delamar, M., 1995, "The Polyimide (PMDA-ODA) Titanium Interface. 2. XPS Study of Polyimide Treatments and Aging," *Journal of Electron Spectroscopy and Related Phenomena*, **74**(1), pp. 57-66.

[22] DeIasi, R., 1973, "Hydrolytic Stability of Polyalkane Imide," *Journal of Applied Polymer Science*, **17**(2), pp. 659-62.

[23] Harper, B.D., and Rao, J.M., 1994, "Some Effects of Water Immersion of the Mechanical Behavior of a Polyimide Film," *ASME Journal of Electronic Packaging*, **116**, pp.317-9.

[24] IPC, 1996, "IPC-6011: Generic Performance Specification for Printed Boards."

[25] IPC, 1988, "IPC-6013: Qualification and Performance Specifications for Flexible Printed Boards."

[26] IPC, 1998, "IPC-6015: Qualification and Performance Specification for Organic Multichip Module (MCM-L) Mounting and Interconnecting Structures."

[27] IPC, 1999, "IPC-6016: Qualification and Performance Specification for High Density Interconnect (HDI) Layers or Boards."

[28] IPC, 1998, "IPC-6018: Microwave End Product Board Inspection and Test."

[29] Bodo, P., and Sundgren, J.E., 1988, "Ion Bombardment and Titanium Film Growth on Polyimide," *Journal of Vacuum Science & Technology A (Vacuum, Surfaces, and Films)*, **6**(4), pp. 2396-402.

[30] Girardeaux, C., Chambaud, G., and Delamar, M., 1996, "The Polyimide (PMDA-ODA) Titanium Interface. 3. A Theoretical Study," *Journal of Electron Spectroscopy and Related Phenomena*, **77**(2), pp. 209-20.

[31] Ho, P.S., et al, 1991, "Chemistry, Microstructure, and Adhesion of Metal-Polymer Interfaces," *Fundamentals of Adhesion*, ed. Lieng-Huang Lee, Plenum Press, New York, pp.383-406.

[32] Ohuchi, F.S., and Freilich, S.C., 1986, "Metal Polyimide Interface: A Titanium Reaction Mechanism," *Journal of Vacuum Science & Technology A (Vacuum, Surfaces, and Films)*, **4**(3), pp. 1039-45.

[33] Jensen, J.J., Cummings, J.P, and Vora, H., 1984, "Copper/Polyimide Materials System for High Performance Packaging," IEEE Transactions on Components, Hybrids, and Manufacturing Technology, **CHMT-7**(4), p. 384-93.

[34] Pottiger, M.T., Coburn, J.C., and Edman, J.R., 1994, "The Effect of Orientation on Thermal Expansion Behavior in Polyimide Films," *Journal of Polymer Science, Part B: Polymer Physics*, **32**(5), pp. 825-37.

[35] Czornyj, G., et al, 1997, "Polymers in Packaging," *Microelectronics Packaging Handbook, Part II: Semiconductor Packaging*, 2nd edition, ed. R.R. Tummala, E.J. Rymaszewski, and A.G. Klopfenstein, Chapman & Hall, New York, pp. 509-623.

[36] DuPont, 2001, "DuPont Kapton E," document H-78305.

[37] Li, M.J., et al, 1995, "Relative Humidity Cycle Testing on GE-HDI," *International Journal of Microelectronic Packaging*, **1**, pp. 13-34.

[38] Sutton, R.F., 1998, "Hygroscopic Expansion of Polyimide Film," IPC Printed Circuits Expo, Long Beach, CA.

[39] Buchhold et. al., 1998, "Influence of Moisture-Uptake on Mechanical Properties of Polymers used in Microelectronics," *Materials Research Society Symposium Proceedings*, **511**, pp. 359-364.

[40] Melcher, J., Daben, Y., and Arlt, G., 1989, "Dielectric Effects of Moisture in Polyimide," *IEEE Transactions on Electrical Insulation*, **24**(1), pp. 31-8.

[41] Lam, D.C.C., Yang, F., and Tong, P., 1999, "Chemical Kinetic Model of Interfacial Degradation of Adhesive Joints," *IEEE Transactions on Components and Packaging Technology*, **22**(2), pp. 215-20.

[42] Popelar, S.F., Popelar, C.H., and Kenner, V.H., 1993, "Time-Dependent Fracture of Polyimide Films," *Transactions of the ASME: Journal of Electronic Packaging*, **115**(3), pp. 264-9.

[43] Pecht, M, and Wu, X., 1994, "Characterization of Polyimides Used in High Density Interconnects," *IEEE Transactions on Components, Packaging, and Manufacturing Technology*, Part B, **17**(4), pp. 632-9.

[44] Popelar, S.F., C.H. Popelar, and V.H. Kenner, 1993, "Hygothermal Effects on the Fracture of Polyimide Film, *ASME Advances in Electronic Packaging*, **4(**1), p.287-94.

[45] Zumdahl, S.S., "Chemical Kinetics," *Chemistry*, Third Edition, D. C. Heath and Co., Lexington, MA, pp. 543-93.

[46] ASTM, 1996, "D1708-96: Standard Test Method for Tensile Properties of Plastics By Use of Microtensile Specimens."

[47] Neves, B., 2001, "Flexible Testing: Don't Be A Test Dummy," *The Board Authority*, March 2001, pp.70-2.

LIST OF FIGURE CAPTIONS

Figure 1. Peel testing of metallization strips deposited on a polyimide substrate using a Dage Microtester 22 machine.

Figure 2. Fit of peel strength regression model, Eq. (4), to experimental data from peel tests. Error bars represent +/- one standard deviation.

Figure 3. Overlaid stress-strain curves for samples aged at 300°C/1%RH. Stars indicate the average failure point for tests conducted following each indicated duration of aging.

Figure 4. Fit of normalized ultimate tensile strength regression model, Eq. (7), to experimental data from tensile tests. Error bars represent +/- one standard deviation.

Figure 5. Factors contributing to deadhesion of polyimide dielectric.

Figure 6. Deadhesion test flow for products where adequate aging can not be practically obtained through prolonged dwells within the temperature/humidity cycling test.

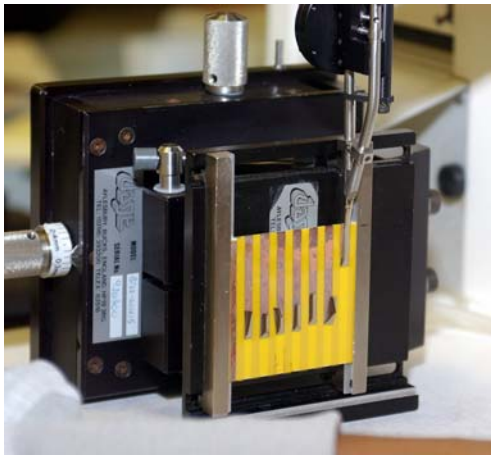

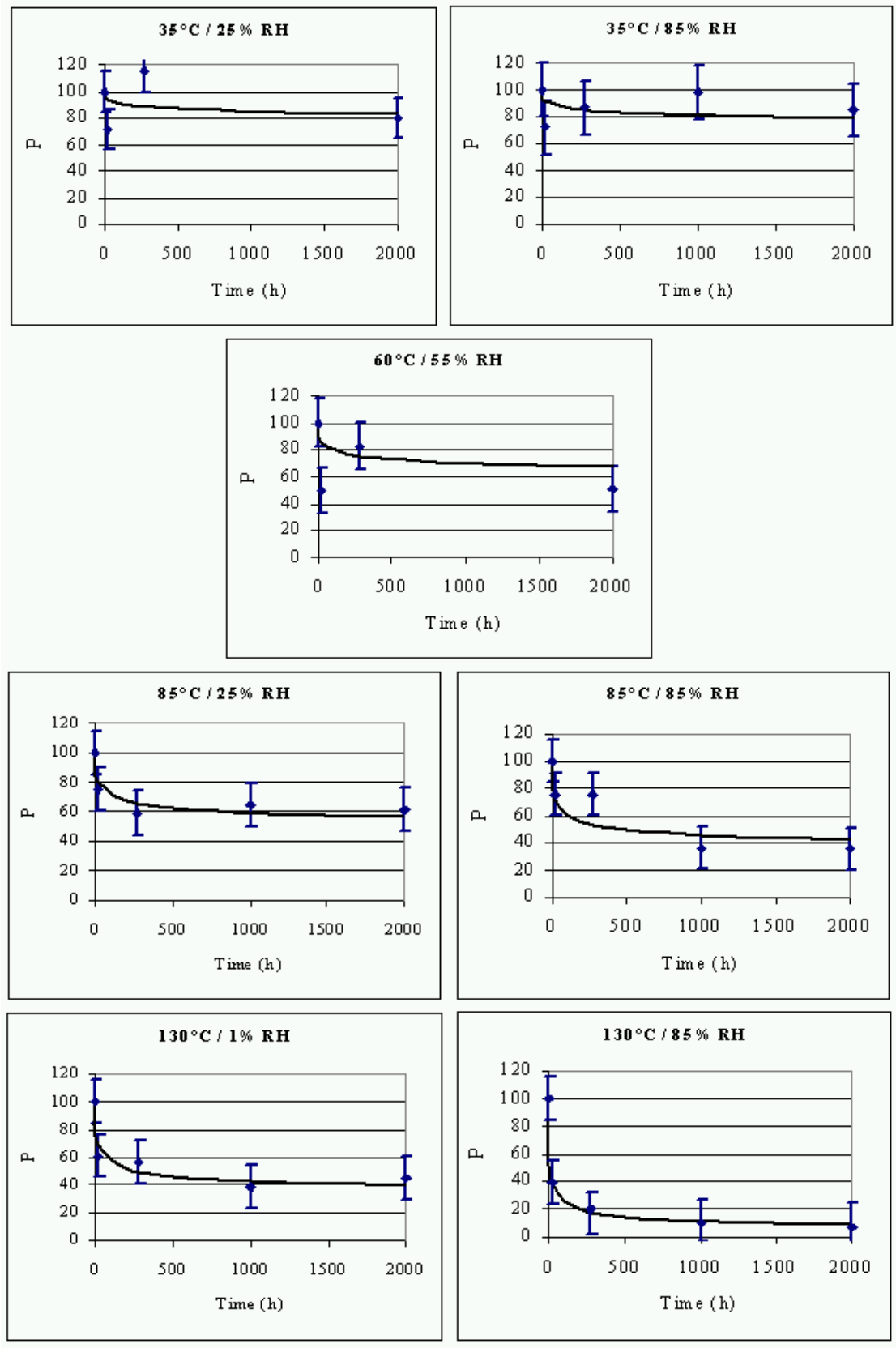
35°C / 25% RH
35°C / 85% RH
60°C / 55% RH
85°C / 25% RH
85°C / 85% RH
130°C / 1% RH
130°C / 85% RH
P
Time (h)
0
20
40
60
80
100
120
500
1000
1500
2000

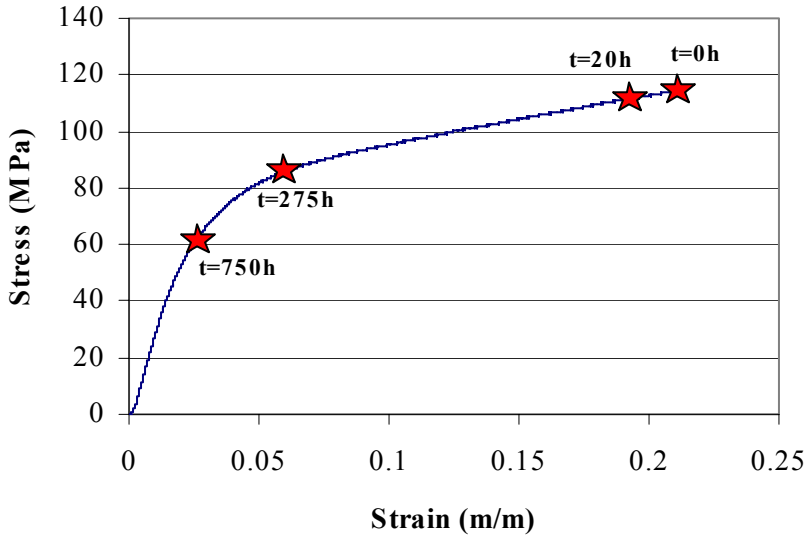
140
120
100
80
60
40
20
0
Stress (MPa)
0
0.05
0.1
0.15
0.2
0.25
Strain (m/m)
t=0h
t=20h
t=275h
t=750h

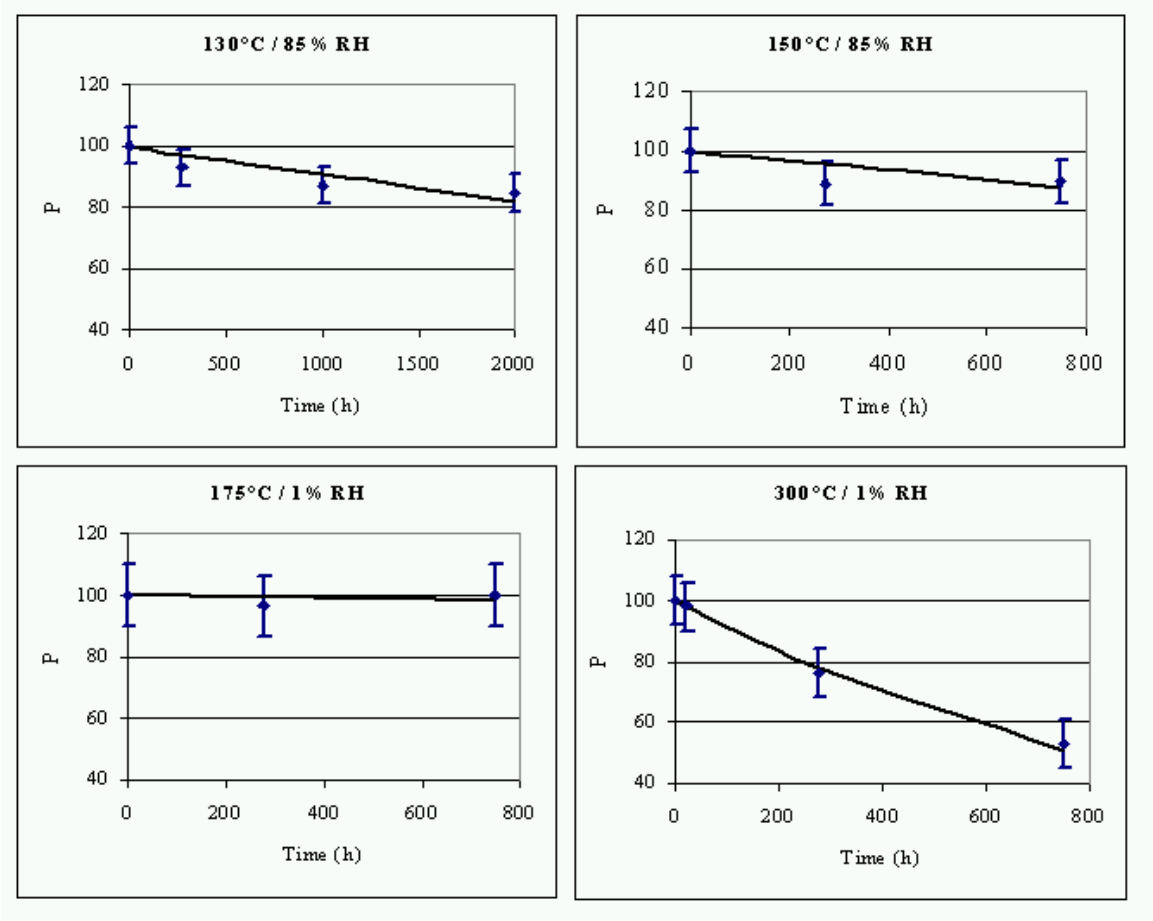
130°C / 85 % RH
120
100
80
60
40
P
0
500
1000
1500
2000
Time (h)
150°C / 85% RH
120
100
80
60
40
P
0
200
400
600
800
Time (h)
175°C / 1% RH
120
100
80
60
40
P
0
200
400
600
800
Time (h)
300°C / 1% RH
120
100
80
60
40
P
0
200
400
600
800
Time (h)

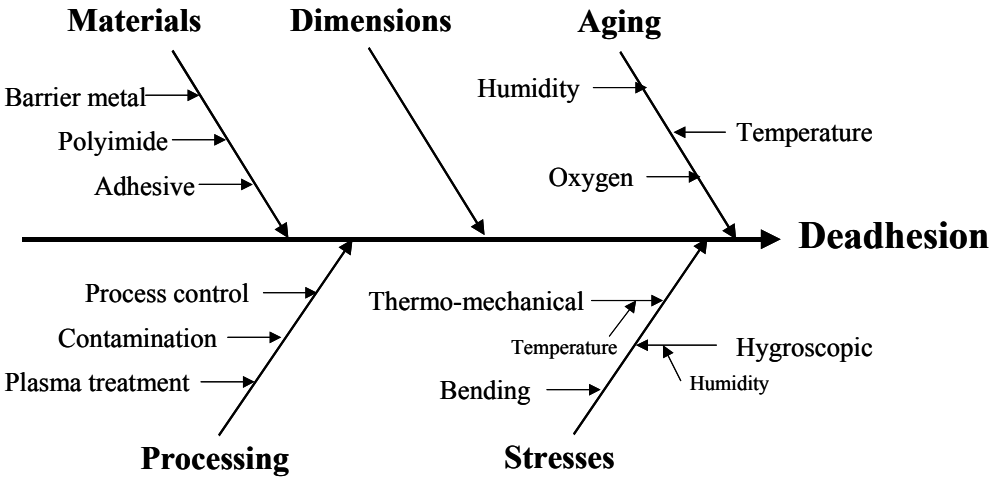
Materials
Dimensions
Aging
Barrier metal
Polyimide
Adhesive
Humidity
Temperature
Oxygen
Deadhesion
Process control
Contamination
Plasma treatment
Thermo-mechanical
Temperature
Hygroscopic
Humidity
Bending
Processing
Stresses

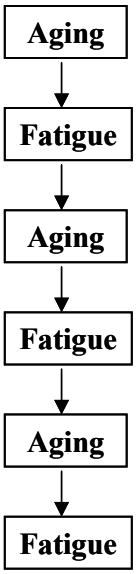

Aging:

- Constant high temperature, high humidity bake. Duration computed using aging model for chosen test conditions.
- Each of the 3 stages generates 1/3 of the aging damage that would be incurred in the application environment.

Fatigue:

- Temperature/humidity cycling. Cycle sizes computed using damage model, if available, or using time compression. If applicable, bending cycles, shocks, and/or vibration can be applied in series with the temperature/humidity cycling.
- Each of the 3 stages applies 1/3 of the loadings that would be experienced in the application environment.